# The Lagrangian Particles in the EM Driven Turbulent Flow with Fine Mesh (the Treatment of *solidParticle* Library in OpenFOAM)

Mihails Ščepanskis and Andris Jakovičs

Laboratory for Mathematical Modelling of Environmental and Technological Processes, University of Latvia
Zellu str. 8, LV-1002, Riga (Latvia)
phone: +371 67033780, fax: +371 67033781
mihails.scepanskis@lu.lv

The paper contains the description of the further development of particles libraries in OpenFOAM in fine near-wall cells. We simulate the flow of induction crucible furnace (ICF) with high Reynolds number. In this case the motion of liquid metal is governed by the Lorenz force and the penetration depth of electromagnetic field is relatively small. For this type of flow and some others it is important to use very fine mesh near the walls. At the same time we simulate the motion of the solid particles in such flow. It is associated with such industrial processes as the impurity depositions on the wall of furnaces, the erosion of the walls and homogenization of the alloying particles. In many cases we have the particles with size more than the size of the cell of the mesh near the wall.

The Lagrangian algorithm for the simulation of the solid particles is already implemented in *solidParticle* library in *OpenFOAM*. But unfortunately it does not simulate the collision of the particle with the wall in the case when the size of the particle is more than the size of the cell. We modified *solidParticle* and *lagrangian* libraries to simulate the collision with the wall correctly.

These modifications give us an opportunity to obtain the results that correspond to industrial and experimental observations in the case of admixture particles in ICF, whereas the standard algorithm of *solidParticle* library gives the non-physical results.

Lagrangian equation in *move* function in *solidParticle* library is also supplemented with EM, lift, acceleration and added mass forces. The new equation considers the non-linearity that forces us to complicate the solution. The results of the admixture particle motion using treated *solidParticles* library are presented in the paper.

## Introduction

We consider the mass transport processes in the metal melts in induction crucible furnaces (ICF). The scheme of the industrial ICF and its simplified model are shown on the Fig. 1. Electromagnetic heating and melting is one of the most effective methods for conducting material processing and production. The melt flow in induction furnaces is formed by Lorentz forces and usually consists of several recirculated vortices. Depending on material properties different types of induction furnaces are suitable for production of high purity metal alloys, ceramics and glasses. Such materials often have very high melting temperature and are not transparent. Thus experimental measurements of particle motion and mass transfer processes are very difficult and even impossible. Computer modelling allows to study parameters of induction equipment and choose optimal parameters of admixture particles before it is built and to improve energy efficiency of melting and homogenization processes.

The problem of solid particle tracking in metal melts is associated with different industrial processes. The alloying particles (such as Mo, Ni, Si etc.) are mixed into the steel melt to increase some properties, such as strength, hardness, wear resistance and others. In this case the goal is to reach the homogeneous distribution of the particles in the short time. The other problem is associated with the impurities that come to the melt from the dirty melting material (such as $SiO_2$, MgO etc.) and from the erosion of the furnace wall (such as $Al_2O_3$). These particles can deposit on the wall of the furnace and change the configuration of the flow and the electromagnetic (EM) field.

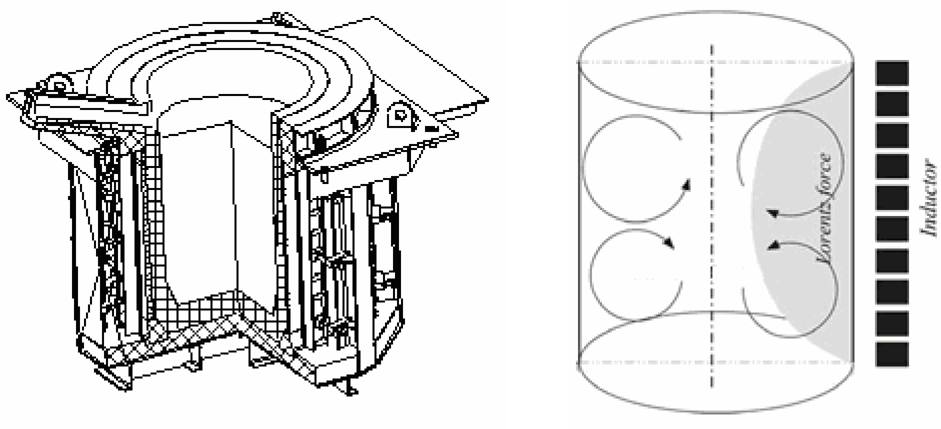


(a) (b)

Fig. 1. The design of industrial ICF (a) and its simplified model with the sketch of the typical vortices of the mean flow (b).

The melt flow consists of several recirculated vortices and is described with high Reynolds number. Thus we should use very fine mesh near the wall to simulate non-stationary turbulent flow. The velocity of the average flow is shown on the Fig. 2 in the central vertical plane of the ICF. There are significant velocity gradients near the wall in the zones of the vortices. Industrial observations show that there can be quit big impurity particles in the melt. So it is important to simulate the collision of the particles with the wall correctly and take into account their size.

But unfortunately the algorithm implemented in *solidParticle* library does not simulate the collision of the particle with the wall in the case when the size of the particle is more than the size of the cell. The standard algorithm in *solidParticle* library indicates the collision only with the faces which are associated with the cell that consider the center of the particle. Thus when the size of particle is more than the size of the cell near the wall it can approach the wall until the center of the particle will not reach the boundary cell. The modification of the libraty that treated this effect is presented in this paper.

## The Treatment of the Algorithm

The scheme of the common algorithm is shown on Fig. 3. The first step of numerical algorithm is the fluid velocity field calculation using Large Eddy Simulation (LES) method; the second one is the particles motion simulation. Both steps are implemented at each time step.

We consider particle transport model with several assumptions made:

- the particle-particle interaction is negligible,
- all particles are rigid spheres,
- the particles do not affect the structure and the velocities of the flow.

Particles are moved by *move* function in *solidParticle* library. The block scheme of the algorithm is shown on Fig. 4. First of all the algorithm define faces that particle can cross or hit using *findFaces* function from *lagrangian* library. If calculated trajectory of the particle remains inside the cell then the particle is simply moved to the end position. If the particle crosses internal face then the particle is moved to the face, the cell is changed and the particle is moved to the end position. If the particle hits a wall then the particle is moved to the wall, the velocity is changed and particle is moved to the end position.

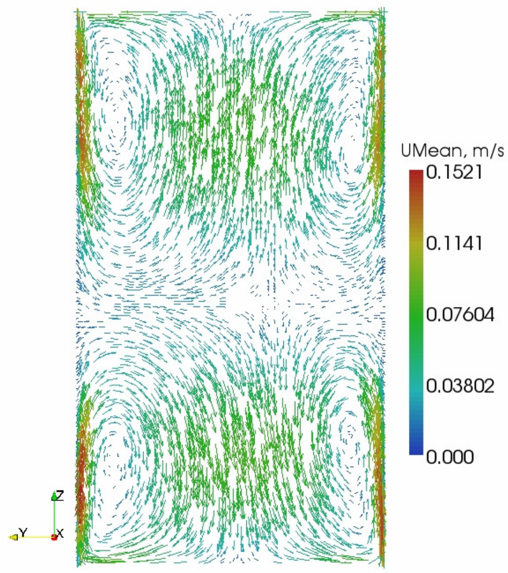


Fig. 2. The velocity of the average flow in the central vertical plane of the ICF.

*findFaces* function search the faces that can be hit or crossed among the faces that are connected with the cell where is the particle. Thus this function can not indicate the collision with the wall if the particle size is bigger than the cell size. It is impossible just to expand the sphere of analysis of *findFaces* function because of the algorithm of the collision indicating. We added the *wallHitChech* code to the algorithm after *findFaces* function (Fig. 4). This code finds the faces that are hit among all boundary faces using special algorithm and adds these faces to the face list.

The *lambda* function from *lagrangian* library is used for the collision indicating. This function also checks if the size of the particle is smaller than the size of the cell and virtually move the wall to the distance of the radius of the particle. Than the collision of the particle centre with this virtual wall is indicated. We removed the check of the particle size from this function to use it in *wallHitCheck* code.

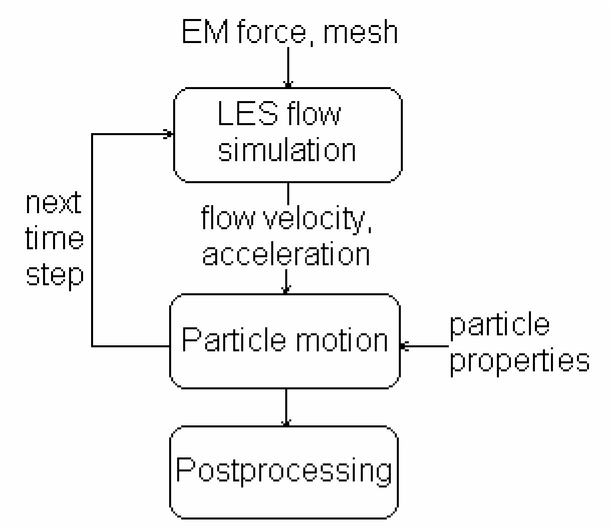


Fig. 3. The scheme of the common algorithm.

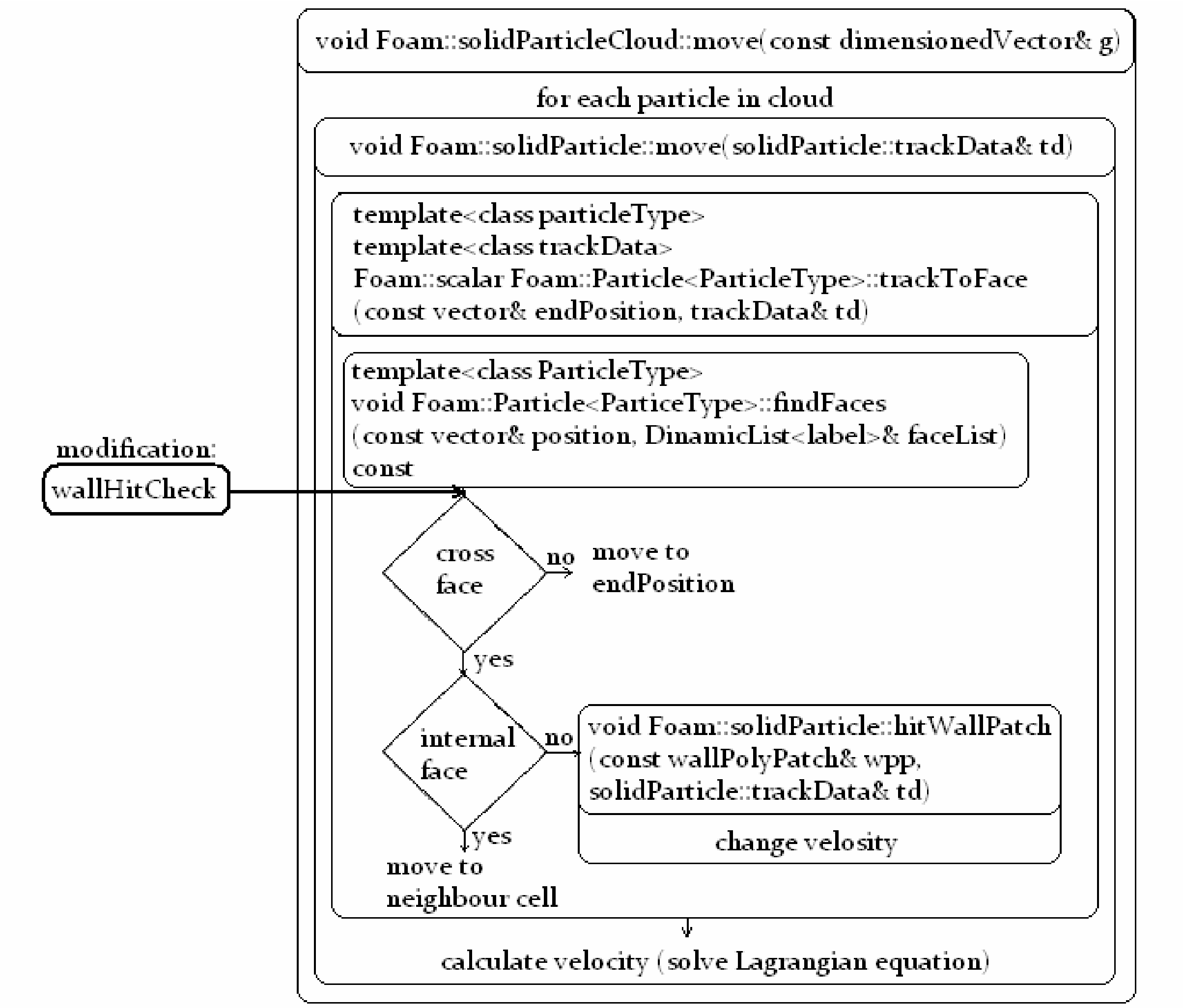


Fig. 4. The algorithm of particle tracking and its modification.

## Development of the Lagrangian Algorithm

The Lagrangian algorithm in *solidParticle* library takes into account only drag and buoyancy forces:

$$\frac{d\mathbf{u_p}}{dt} = C_D \cdot \mathbf{U} + \left(1 - \frac{\rho_f}{\rho_p}\right) \cdot \mathbf{g},$$

where drag coefficient is in Schiller-Naumann approximation [1]

$$C_D = \frac{18\nu}{d^2} \frac{\rho_f}{\rho_p} \cdot \left(1 + 0.15 \cdot \mathrm{Re}_p^{0.687}\right)$$

if $\mathrm{Re}_p > 1$ and $C_D = 1$ otherwise; $\mathrm{Re}_p = dU/\nu$ is particle Reynolds number, $\mathbf{U} = \mathbf{u_f} - \mathbf{u_p}$ is relative particle velocity ($\mathbf{u_f}$ and $\mathbf{u_p}$ are liquid and particle velocities respectively), $d$ is particle diameter, $\nu$ is kinematic viscosity, $\rho_f$ and $\rho_p$ are liquid and particle densities respectively, $\mathbf{g}$ is free fall acceleration.

Previously we have proved that the electromagnetic (EM), lift, acceleration and added mass forces are also significant in considerable problem [2, 3]. Thus the Lagrangian equation should be so [3]:

$$\left(1+\frac{C_A}{2}\frac{\rho_f}{\rho_p}\right)\cdot\frac{d\mathbf{u_p}}{dt}=C_D\cdot\mathbf{U}+\left(1-\frac{\rho_f}{\rho_p}\right)\cdot\mathbf{g}-\frac{3}{4}\frac{1}{\rho_p}\mathbf{f_{em}}+\frac{\rho_f}{\rho_p}C_L\boldsymbol{\xi}+\left(1+\frac{C_A}{2}\right)\cdot\frac{D\mathbf{u_f}}{Dt},\quad(1)$$

where the Odar-Hamilton approximation for acceleration coefficient $C_A$ [4] and the Legendre-Magnaudet approximation for the lift coefficient $C_L$ [5] are used:

$$C_A=2.1-\frac{0.132}{0.12+Ac^2},$$

$$C_L(\mathrm{Re}_p)=\frac{1}{2}\frac{1+16\cdot\mathrm{Re}_p^{-1}}{1+29\cdot\mathrm{Re}_p^{-1}};$$

$Ac=U^2\big/a\dot{U}$ ($\dot{U}$ is relative acceleration) is acceleration parameter; vector $\mathbf{f_{em}}=[\mathbf{j}\times\mathbf{B}]$ is the Lorentz force density, $\mathbf{j}$ is a current density, $\mathbf{B}$ is magnetic field induction; vector $\boldsymbol{\xi}=[\mathbf{U}\times[\nabla\times\mathbf{U}]]$ describes the lift force.

Equation (1) is non-linear, so some variables are taken from previous time step and linearized equation is solved numerically using the implicit difference scheme. Thus we get the system of linear algebraic equation for vector $\mathbf{u_p}$ components. This system is solved using Gauss method. To guarantee the convergence of the method we separate the time step for LES solver to smaller time steps for the Lagrangian equation.

## The Results Obtained Using Different Models

Three different models of the behaviour of the particles close to the wall are analyzed: from simple standard algorithm of the *solidParticle* library to sophisticate treated code described above.

*Model 1.* Non-treated algorithm of *solidParticle* library is used in this model. For the particles with size bigger than cell size the size of the particle is neglected in the case of collisions with the wall. Equation (1) is used for calculation of the particle velocity.

*Model 2.* This model corresponds to the simple modification of the standard algorithm. The particle is moved to the distance of the radius from the wall if it is closer at the end of algorithm each time step. This model can not be generalized for any sophisticate geometry.

*Model 3.* This model uses treated algorithm described above and correctly takes into account size of the particles.

The results that were obtained using *Models 1-3* are shown on Fig. 5-7 respectively. The diameter of the particles ranges between 0.1 and 1.9 mm. The mesh with 2.8 million nodes was used. The smallest cells are cells near the boundary, they are 0.1 mm thin. The particles are input into the developed turbulent flow of the melt at the horizontal plane 1.5 cm deep from the top surface of the crucible. Such the initial position corresponds to the industrial case.

In all models the most heavy particles (Fig. 5-7 (c)) come to the bottom. Only the small particles move in the flow due to drag force. The results of *Model 1-3* are qualitatively similar in this case.

But for the case of the light particles and the case of the particle with density equal to liquid density the results that were obtained using *Model 1-3* are significantly different.

Using *Model 1* we obtain the result that big particles with the density equal to the liquid density are concentrated on the wall near the top surface of the crucible (Figure 5 (b),(e)). In this model the size of the particle is not taken into account, thus the particle can come near the wall where, due to non-slip boundary condition the flow velocity magnitude is negligible, thus the particle stay in this region near the wall. The light particles concentrate on the top surface near the wall. This result corresponds to the industrial observation of the “slag” formation [6].

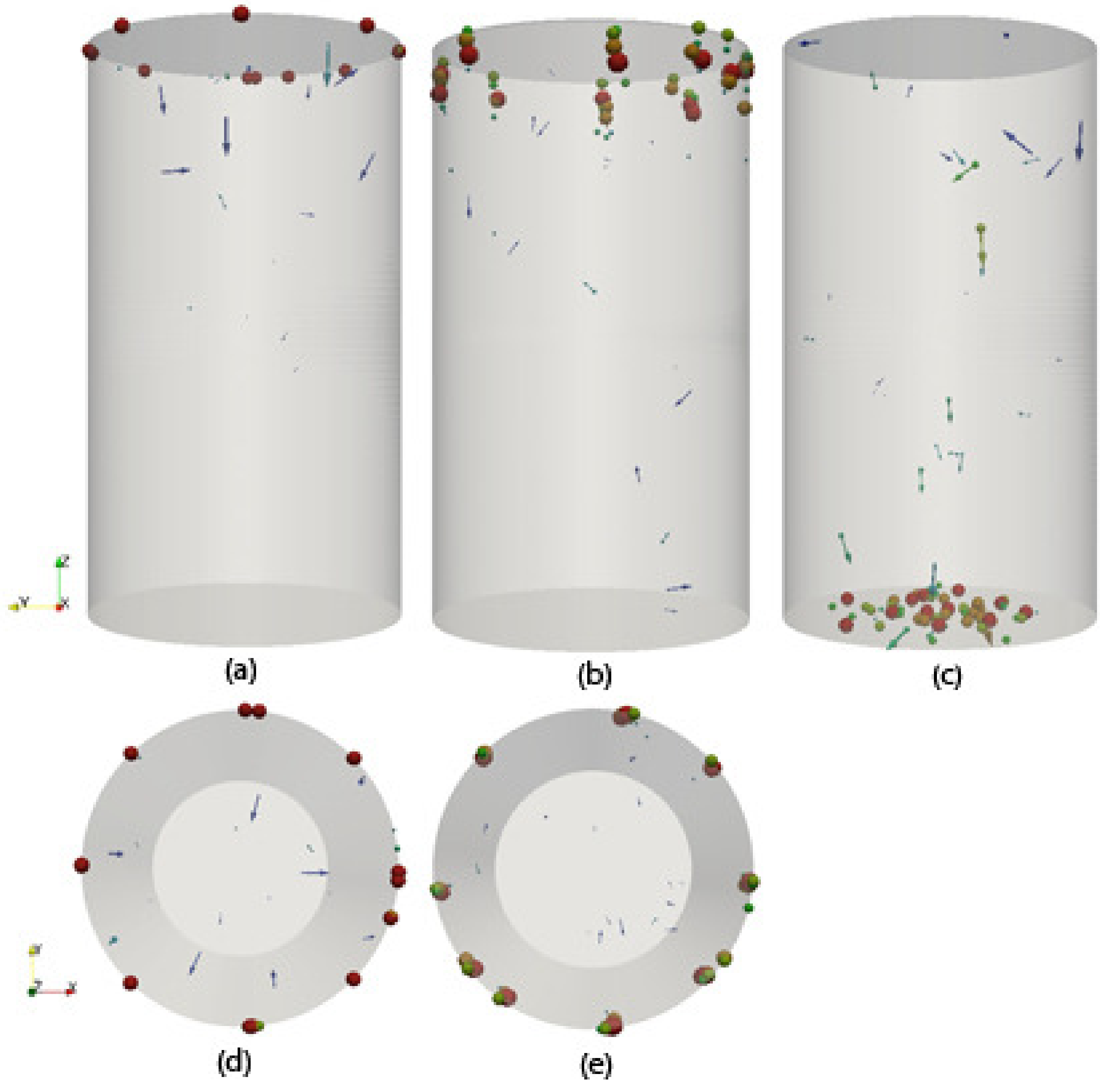


Fig. 5. The positions of the particles in ICF after 10 s from the moment when they was input. Calculated using *Model 1*. (a), (d) - $\rho_p = \rho_f / 1.5$, (b), (e) - $\rho_p = \rho_f$, (c) - $\rho_p = 1.5 \cdot \rho_f$. The arrows show the direction and the magnitude of the momentary particle velocity at the 10 s. The images are drawn with respect to the optical perspective.

*Model 2* gives us another result: big particles are rapidly concentrated near the wall in the middle of the crucible (Figure 6 (a), (b), (d), (e)). The middle zone of the crucible is the zone between two eddies of the averaged flow (Figure 2). The magnitude of the velocity of the flow in this zone is small (Figure 2) and EM force is comparatively great in this zone near the wall. Thus big particles are concentrated near the wall in the zone between two eddies. The physical model of the behaviour of the particles and their concentration in the middle zone near the wall described in [7]. Such a situation is also observed in the experimental investigations of the other authors (e. g. [8]).

The results that were obtained using *Model 3* are shown on Fig. 7. These results are physically more realistic. Big light particles form the “slag” like in the *Model 1* and industrial observation [6]. Smaller particles move by the wall and concentrates in the middle zone of the crucible as in experimental observation [8] but not so rapidly like in results of *Model 2*. Thus

*Model 3* explains both experimental and industrial phenomena but previous models do not do this simultaneously.

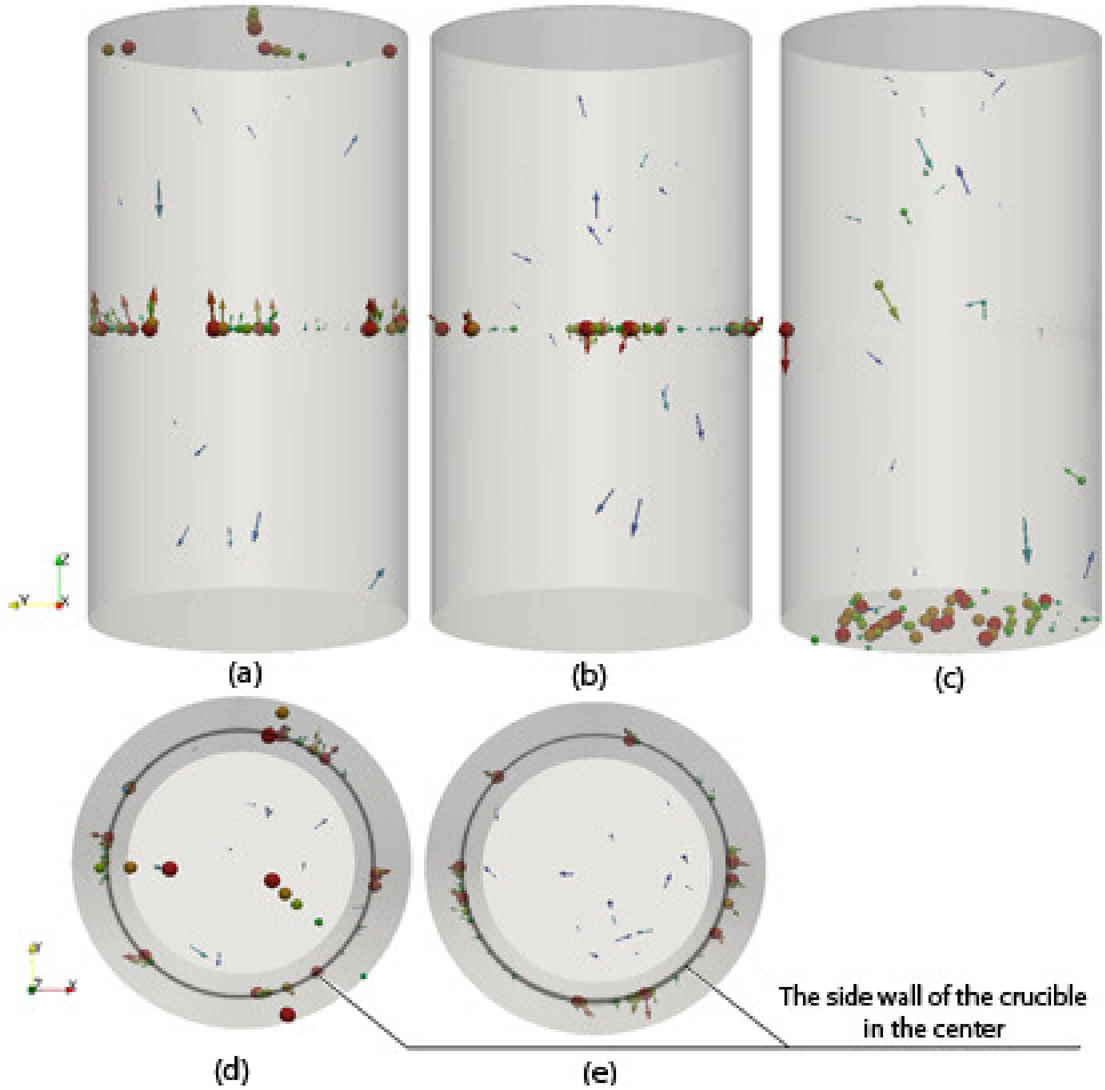


Fig. 6. The positions of the particles in ICF after 10 s from the moment when they was input. Calculated using *Model 2*. (a), (d) - $\rho_p = \rho_f / 1.5$, (b), (e) - $\rho_p = \rho_f$, (c) - $\rho_p = 1.5 \cdot \rho_f$. The arrows show the direction and the magnitude of the momentary particle velocity at the 10 s. The images are drawn with respect to the optical perspective.

The origin of the significant difference in the results is the particle behaviour near the top surface and the wall of the crucible. The simplified scheme of the motion of the particle cloud in the turbulent flow of ICF is shown on Fig. 8 [3].

Initially all particles are going by the top surface to the wall and then down through the zone of the upper eddy near the wall to the middle part. Then the cloud of the particles separates: one part goes to the zone of the upper eddy and other part to the zone of the lower eddy. After that the particle exchange between two eddies decreases the difference between the number of the particles in zones of the upper and the lower eddies with the lapse of time.

Different models calculate the trajectory of the particles in the zone of the corner between the top surface and the wall quite differently. *Model 1* allows the particle center reach the wall where the flow velocity is negligible, thus the particle remains in this zone. *Model 2* allows the particle approach the wall closer then the radius and only after that moves it to the distance of the radius in the normal direction from the wall. Thus the particle can move in parallel direction of the wall in this case. But *Model 3* simulate the collision of the particle with the wall correctly, thus the results are more physical.

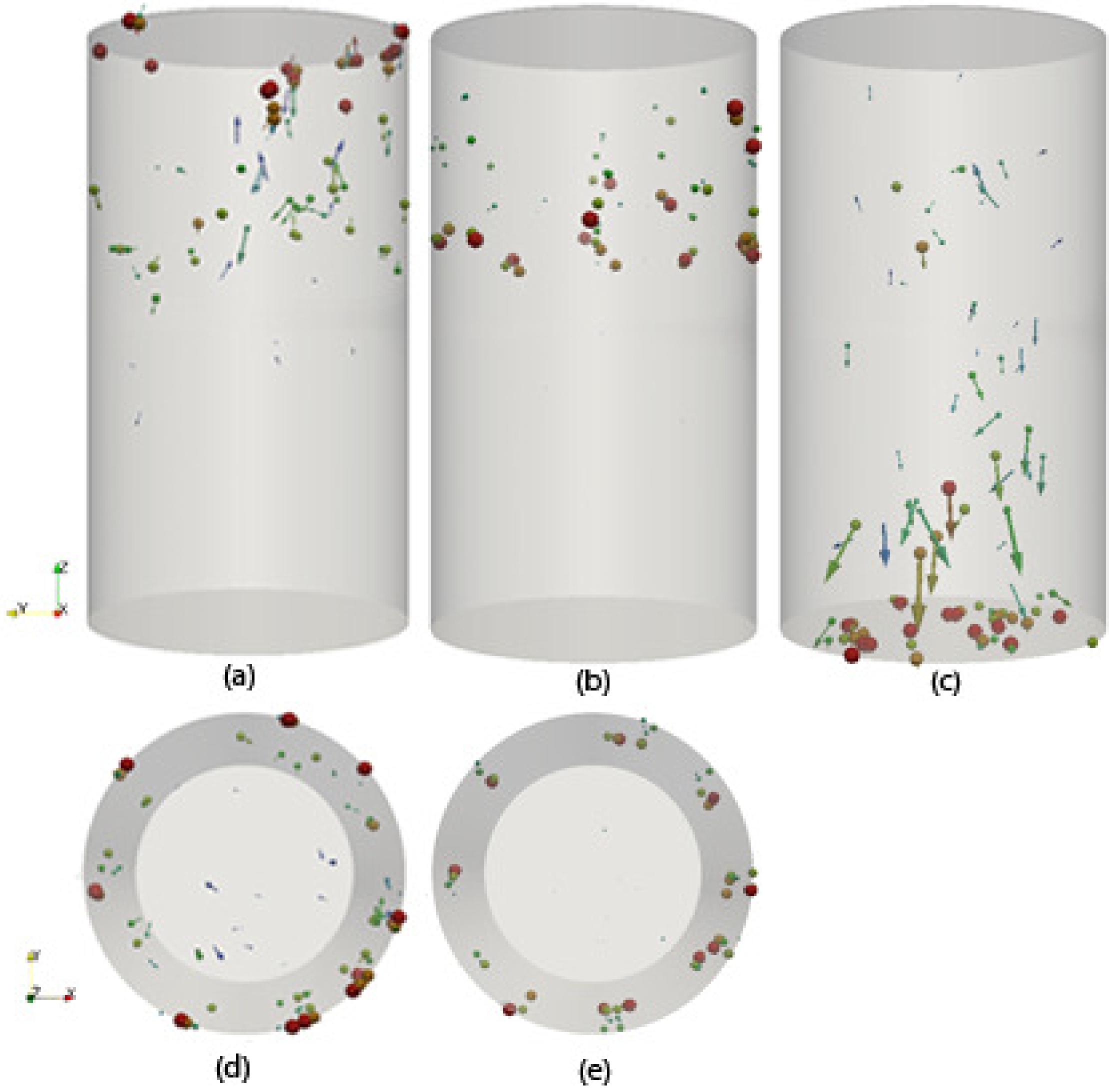


Fig. 7. The positions of the particles in ICF after 7 s from the moment when they was input. Calculated using *Model 3*. (a), (d) - $\rho_p = \rho_f / 1.5$, (b), (e) - $\rho_p = \rho_f$, (c) - $\rho_p = 1.5 \cdot \rho_f$. The arrows (except (b) and (e)) show the direction and the magnitude of the momentary particle velocity at the 7 s. The images are drawn with respect to the optical perspective.

**Consclusions**

The treated algorithm of the *solidParticle* library is developed. This algorithm takes into account the size of the particle in the case when it is bigger then the size of the cell and simulate the collision with the wall correctly. The algorithm is described in this paper.

In the case that corresponds to the industrial input of the alloying particles in the melt of ICF the particle cloud initially goes through the zone of the corner between the top surface and the wall. Only treated algorithm described above simulate the motion of the particles in this zone correctly.

Lagrangian equation in *move* function in *solidParticle* library was also supplemented with EM, lift, acceleration and added mass forces.

The treated algorithm gives the results that correspond to the industrial and experimental observations: “slag” formation and deposition of big particles on the wall mainly in the middle zone of the crucible.

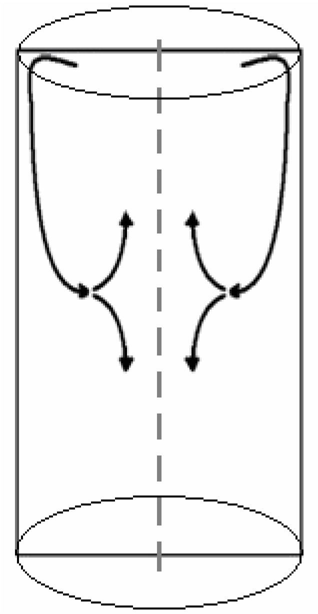

Fig. 8. The simplified scheme of the motion of the particle cloud in ICF when they are input on the plane near the top surface like in the industrial case.

**Acknowledgements**

The part of described algorithm was developed using the idea by Dr. Niklas Nordin from Scania CV AB and the authors thank him for support. Also this work has been supported by the European Social Fund (ESF).

**References**

[1] L. Schiller and Z. Naumann, Uber die grundlegenden berechnungen bei der schwerkrafttaufbereitung (in Germany), *Ver. Deut. Ing.*, **77**, pp. 318-320 (1933)

[2] M. Ščepanskis, A. Jakovičs, B. Nacke and E. Baake, The simulation of the behaviour of alloying admixture particles in the induction crucible furnaces, In the Proceeding of the *International Symposium on Heating by Electromagnetic Sources,* Padua, Italy, pp. 3-10 (2010)

[3] M. Ščepanskis, A. Jakovičs and B. Nacke. The Simulation of the motion of Solid Particles in the Turbulent Flow of Induction Crucible Furnaces. In the Proceeding of the *5th European Conference on Computational Fluid Dynamics* (on CD), Lisbon, Portugal. In the Book of Abstracts: Vol. 1, p. 103 (2010)

[4] F. Odar and W. S. Hamilton, Forces on a sphere accelerating in a viscous fluid, *J. Fluid Mech*, **18**, pp. 302-314 (1964)

[5] D. Legendre and J. Magnaudet, The lift force on a spherical bubble in a viscous linear shear flow, *J. Fluid Mech*, **368**, pp. 81-126 (1998)

[6] E. Dötsch, Inductive melting and holding, *Vulkan-Verlag* (2009)

[7] M. Ščepanskis, A. Jakovičs, B. Nacke, Homogenization of Alloying Particles in Induction Crucible Furnaces, In the Proceeding of the *6th International Scientific Colloquium on Modelling for Material Processing,* Riga, Latvia, pp. 259 - -264 (2010)

[8] M. Higuchi, H. Amabai, S. Shimasaki, C. Kamata, S. Teshigawara, and S. Taniguchi, Electromagnetic separation of inclusions from molten copper by alternating electromagnetic field, In the Proceeding of the *6th International Conference on Electromagnetic Processing of Materials*, Dresden, Germany, pp. 86-89 (2009)